AGU PUBLICATIONS

Paleoceanography

RESEARCH ARTICLE
10.1002/2014PA002700

Key Points:
- Seven regional benthic δ^{18}O stacks with ^{14}C age models
- Termination 1 onset at 18.5 ka in intermediate South Atlantic and 14.5 ka in deep Indian
- Deep Pacific lags deep Atlantic by average of 1 kyr during Termination 1

Supporting Information:
- Readme
- Table S1
- Table S2
- Table S3
- Table S4
- Text S1
- Figure S1
- Figure S2

Correspondence to:
L. E. Lisiecki,
lisiecki@geol.ucsb.edu

Citation:
Stern, J. V., and L. E. Lisiecki (2014), Termination 1 timing in radiocarbon-dated regional benthic δ^{18}O stacks, *Paleoceanography*, *29*, 1127–1142, doi:10.1002/2014PA002700.

Received 15 JUL 2014
Accepted 20 OCT 2014
Accepted article online 24 OCT 2014
Published online 4 DEC 2014

Termination 1 timing in radiocarbon-dated regional benthic δ^{18}O stacks

Joseph V. Stern[1] and Lorraine E. Lisiecki[1]

[1]Department of Earth Science, University of California, Santa Barbara, California, USA

Abstract Benthic δ^{18}O changes are often assumed to be globally synchronous, but studies comparing 2–9 radiocarbon-dated records over the most recent deglaciation (Termination 1) have proposed differences in the timing of benthic δ^{18}O change between the Atlantic and Pacific, intermediate and deep, and North and South Atlantic. Because of the relatively small number of records used in these previous studies, it has remained unclear whether these differences are local or regional in scale. Here we present seven regional benthic δ^{18}O stacks for 0–40 kyr B.P. that include 252 records with independent regional age models constrained by 852 planktonic foraminiferal ^{14}C dates from 61 of these cores. We find a 4000 year difference between the earliest termination onset in the intermediate South Atlantic at 18.5 (95% confidence interval: 17.9–19.0) kyr B.P. and the latest in the deep Indian at 14.5 (14.1–15.0) kyr B.P. The termination onset occurs at 17.5 kyr B.P. in the intermediate and deep North Atlantic, deep South Atlantic, and deep Pacific. However, throughout the termination deep North Atlantic benthic δ^{18}O leads the deep Pacific by an average of 1000 year and a maximum of 1700 year. Additionally, the intermediate Pacific termination onset at 16.5 (16.1–16.9) kyr B.P. demonstrates that intermediate-depth benthic δ^{18}O change was not globally synchronous. These regional stacks provide better age models than a global stack across Termination 1 and potentially important constraints on deglacial ocean circulation changes.

1. Introduction

The δ^{18}O of benthic foraminiferal calcite reflects the combined effects of continental ice volume (sea level), deep water temperature, and the δ^{18}O of seawater at the location of deep water formation, as influenced by evaporation, precipitation, and glacial meltwater. Because benthic δ^{18}O records are similar globally, they are often used to correlate ages between ocean sediment cores on local to global scales. Global δ^{18}O stacks (averages) of aligned δ^{18}O records also provide orbital-scale chronostratigraphic tools with better signal-to-noise ratios than individual records. However, mounting evidence suggests that benthic δ^{18}O is not globally synchronous and, thus, is unsuitable for global-scale correlations during glacial terminations.

High-resolution planktonic ^{14}C age models from two cores indicate that during the middle of the last termination deep Pacific benthic δ^{18}O lagged the deep North Atlantic by 3900 years [*Skinner and Shackleton*, 2005]. Analysis of sedimentation rates from 33 sites suggests an average Pacific lag of 1600 year during the last five terminations [*Lisiecki and Raymo*, 2009]. *Skinner and Shackleton* [2005] proposed that the Pacific lag was due to a delayed temperature response, while several subsequent modeling studies have investigated the role of δ^{18}O transit time [*Wunsch and Heimbach*, 2008; *Ganopolski and Roche*, 2009; *Primeau and Deleersnijder*, 2009; *Siberlin and Wunsch*, 2011; *Friedrich and Timmermann*, 2012; *Gebbie*, 2012].

Other studies have focused on identifying the age at which Termination 1 begins in different regions. *Labeyrie et al.* [2005] found that the termination onset occurred first at intermediate depths in the North Atlantic and Indian Oceans at 17.0 kyr B.P. and then 1000–1500 years later in the deep North Atlantic and Pacific. *Waelbroeck et al.* [2011] identified the benthic δ^{18}O termination onset at 17.5 kyr B.P. in the intermediate North and South Atlantic, 17.0 kyr B.P. in the deep North Atlantic, and 16.0 kyr B.P. in the deep South Atlantic. Vast regions of the ocean are represented by single-core locations in these studies, raising the question of whether the observed age differences in benthic δ^{18}O are truly regional in scale.

In this paper, we fill the void between global stacks and comparisons of individual records by generating seven regional benthic δ^{18}O stacks with independent radiocarbon age models. Compared to previous longer regional benthic δ^{18}O stacks, our new high-resolution stacks are based on many more records, provide improved geographic coverage, and have significantly improved age models [*Labeyrie et al.*, 1987; *Bassinot et al.*, 1994;

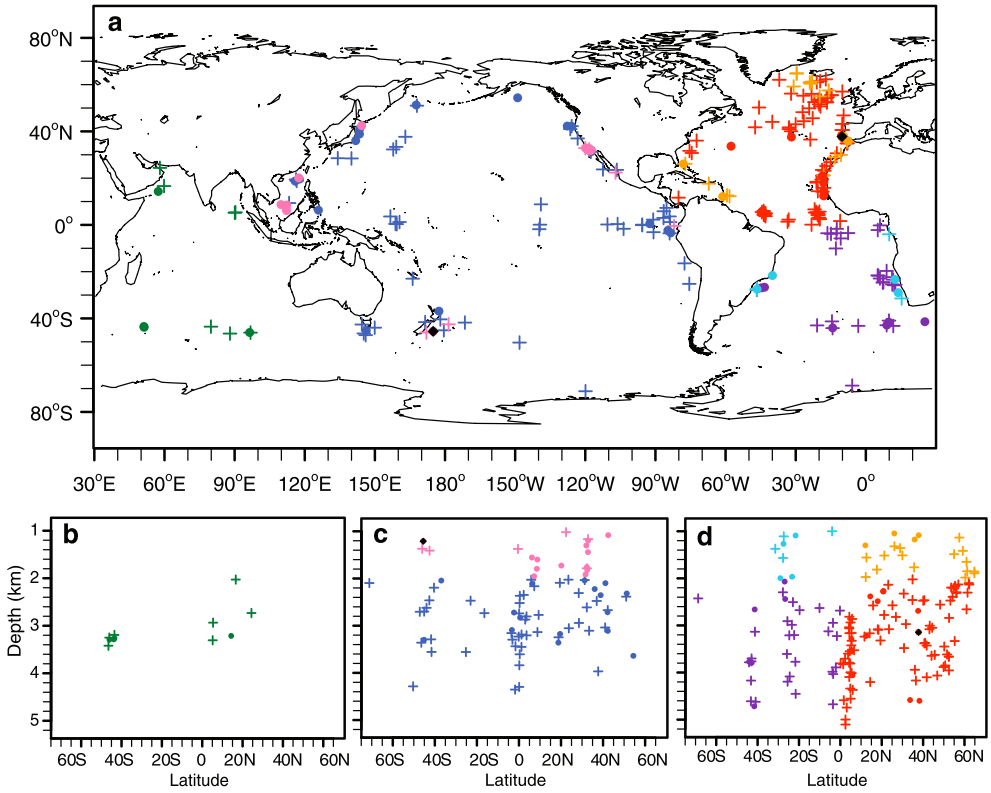

Figure 1. (a) World map showing the locations of cores used in this study and latitude versus depth profiles for the (b) Indian, (c) Pacific, and (d) Atlantic basins. Filled circles indicate cores with radiocarbon dates; crosses mark sites with only benthic δ^{18}O; black diamonds mark the locations of alignment target cores MD95-2042 (Atlantic) and MD97-2120 (Pacific). Green = deep Indian, pink = intermediate Pacific, blue = deep Pacific, orange = intermediate North Atlantic, red = deep North Atlantic, light blue = intermediate South Atlantic, and purple = deep South Atlantic. See Table S1 for a complete list of cores and data references.

Cramer et al., 2009; *Lisiecki and Raymo*, 2009]. These regional stacks provide useful tools for developing stratigraphically aligned age models for cores without high-resolution ^{14}C age models, data for comparison with modeling efforts, and insights into glacial and deglacial climate processes. For example, compilation studies that rely on global-scale δ^{18}O chronostratigraphies can only produce coarse age models appropriate for orbital-scale, but not millennial-scale, applications [e.g., *Oliver et al.*, 2010]. Our regional stacks can be used to test whether the most recent maximum in benthic δ^{18}O was globally synchronous and corresponds to the Last Glacial Maximum (LGM), as commonly assumed for mapping LGM sea surface temperatures [*CLIMAP Project Members*, 1981; *MARGO Project Members*, 2009] and deep water mass boundaries [*Raymo et al.*, 1990; *Curry and Oppo*, 2005]. Regional stacks can also help assess the uncertainty associated with global stacks, which assume globally synchronous δ^{18}O changes [*Imbrie et al.*, 1984; *Pisias et al.*, 1984; *Martinson et al.*, 1987; *Lisiecki and Raymo*, 2005]. Finally, proxy compilation studies that limited themselves to radiocarbon-dated marine records [e.g., *Shakun et al.*, 2012] might include more records if regional benthic δ^{18}O chronologies were available to generate reliable age estimates for cores without ^{14}C dates.

2. Methods

2.1. Overview

Seven different regional stacks are generated using 252 previously published benthic δ^{18}O records and 852 planktonic radiocarbon dates from 61 of those cores (Figure 1 and Table S1 and Figure S1 in the supporting information). Each of the seven stacks has an age model based on combining planktonic ^{14}C measurements from multiple cores within that region by assuming that benthic δ^{18}O is synchronous within each region (but not necessarily between regions). This produces seven regionally averaged age models based on

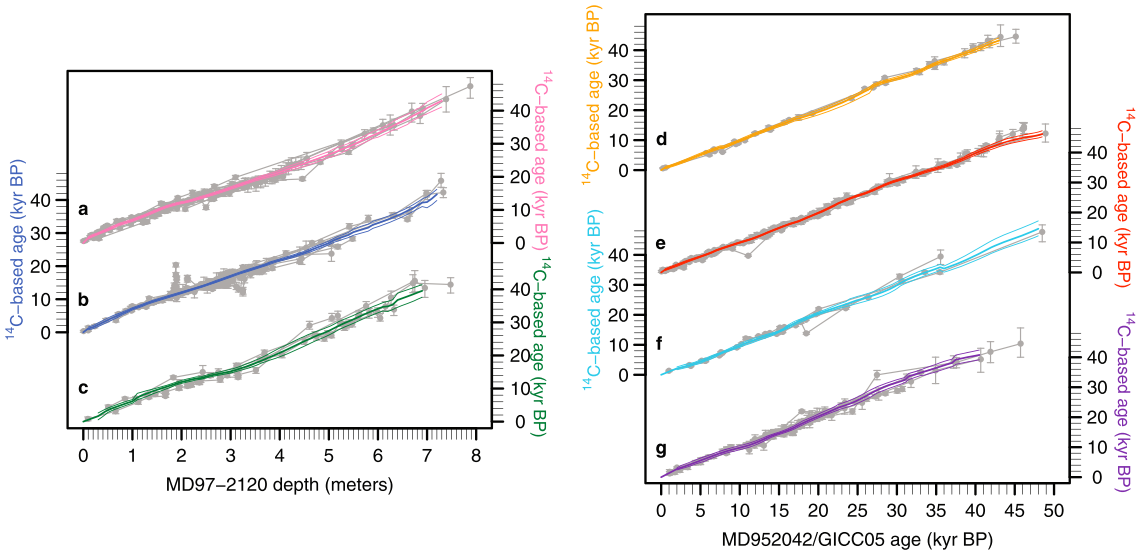

Figure 2. Regional radiocarbon age models for the (a) intermediate Pacific, (b) deep Pacific, (c) deep Indian, (d) intermediate North Atlantic, (e) deep North Atlantic, (f) intermediate South Atlantic, and (g) deep South Atlantic. Gray circles show individual calibrated ^{14}C dates with 95% error bars; gray lines connect dates for individual cores; thick colored lines show the regional age models; thin colored lines indicate the 95% uncertainty bands. In Figures 2a–2c age models and ^{14}C dates from all Pacific cores are plotted relative to MD97-2120 depth based on the alignment of individual benthic δ^{18}O records to MD97-2120. In Figures 2d–2g age models and ^{14}C dates from all Atlantic cores are plotted versus the GICC05 age model based on alignment with MD95-2042. The final age models for each regional stack are based on radiocarbon ages (*y* axis) rather than depth or GICC age (*x* axis).

completely independent sets of ^{14}C dates (Figure 2). We also aligned benthic δ^{18}O from cores without ^{14}C dates to include in the regional stacks, but these records do not contribute to the age models.

Before δ^{18}O values are averaged to create the regional stacks, each benthic δ^{18}O record is placed on its regional radiocarbon age model by converting from aligned target depth to ^{14}C-based calendar years using its regional ^{14}C compilation. Because each region has a different mapping (colored lines in Figure 2) from alignment target (*x* axis) to ^{14}C age (*y* axis) using only ^{14}C dates from that region, the same target depth is matched to a different ^{14}C age depending on a core's region. Thus, benthic δ^{18}O data from each region are assigned a different independent ^{14}C age model.

Our seven regions are the intermediate North Atlantic, deep North Atlantic, intermediate South Atlantic, deep South Atlantic, intermediate Pacific, deep Pacific, and deep Indian (Figure 1). We separated the North and South Atlantic at the equator. An upper boundary of 1000 m was used for the all intermediate stacks (following *Labeyrie et al*. [2005] and *Waelbroeck et al*. [2011]) because shallower benthic δ^{18}O values display a strong gradient with depth due to the influence of the thermocline [*Curry and Oppo*, 2005]. The intermediate and deep stacks are separated at 2000 m based on the previously identified LGM boundary between deep, poorly ventilated southern-sourced waters and better ventilated intermediate waters in all three ocean basins [*Kallel et al*., 1988; *Matsumoto et al*., 2002; *Curry and Oppo*, 2005]. Although previous benthic δ^{18}O comparisons defined depths of 1000–2200 m as intermediate and >3000 m as deep [*Labeyrie et al*., 2005; *Waelbroeck et al*., 2011], we find that our results are not greatly affected by small shifts in the boundary between our intermediate and deep regions.

2.2. Regional ^{14}C Age Models

An initial radiocarbon age model was generated for each of the 61 dated cores using that core's radiocarbon dates, the Bayesian age modeling software Bacon [*Blaauw and Christen*, 2011], the Marine13 calibration [*Reimer et al*., 2013], and constant 405 ^{14}C yr reservoir ages. Bacon was used to estimate the ages of specified depths throughout each radiocarbon-dated core, including robust Monte Carlo uncertainty estimates that increase with distance from ^{14}C dates.

In order to transfer age estimates between cores within each region, we next aligned all the Atlantic benthic δ^{18}O records to MD95-2042 [*Shackleton et al*., 2000] and all the Indian and Pacific records to MD97-2120

[*Pahnke and Zahn*, 2005] using the automated alignment software Match [*Lisiecki and Lisiecki*, 2002]. We refer to these two reference records as alignment "targets." We chose two targets because (1) Atlantic/Pacific benthic δ^{18}O differences have been shown using a fairly large number of records [*Lisiecki and Raymo*, 2009]; (2) there are few records from the Indian Ocean, and we expected Indian benthic δ^{18}O to be similar to that of the Pacific; and (3) having a single Atlantic target allowed us to easily investigate different boundaries for the Atlantic regions (similarly for the Pacific). Sensitivity to choice of alignment targets is discussed in section 4.1.

The intermediate Pacific provides an example to illustrate how we combined our benthic δ^{18}O alignments with the Bacon-generated radiocarbon age models for individual cores to make a regionally averaged ^{14}C age model. In this case, the Indo-Pacific target core MD97-2120 is from the intermediate Pacific, and there are 13 additional dated cores from this region. First, we aligned benthic δ^{18}O from each of these 13 other intermediate Pacific cores to MD97-2120 on its depth scale. Second, we used Bacon to generate calibrated age estimates for MD97-2120 (based only on dates from MD97-2120) at evenly spaced 10 cm intervals. Third, we used our benthic δ^{18}O alignments to convert from these same evenly spaced 10 cm depth intervals in MD97-2120 to the corresponding unevenly spaced depths in each core. Fourth, we used Bacon to generate age estimates from each of the 13 individual core's radiocarbon age models at these depths.

Finally, the intermediate Pacific age model was constructed as the regional average of Bacon-generated age estimates every 10 cm on the aligned-to-MD97-2120 depth scale (Figure 2a). Thus, the average age at these 10 cm target intervals is estimated by averaging the Bacon ^{14}C age estimates from all intermediate Pacific cores that span a particular portion of the record. Not all cores have benthic δ^{18}O and planktonic ^{14}C dates over the entire range of the age models. For example, the intermediate Pacific age model is based on averaging age estimates from seven cores at 1.0 m (based on alignment to MD97-2120 depth) and from twelve cores at 3.0 m (MD97-2120 depth). We only calculate a regional age model for aligned depths that are spanned by at least two cores with radiocarbon age estimates, and we fix all the age models at 0 kyr B.P. Our choice of 10 cm depth spacing in MD97-2120 corresponds to an average of about 600 years on the intermediate Pacific age model.

Age model development for the deep Indian and deep Pacific followed the same methodology as described for the intermediate Pacific, except that only ages from cores located within these regions were used. Radiocarbon measurements from the alignment target (MD97-2120) are included in the intermediate Pacific age model and are equally weighted with dates from other cores in the region. Age estimates from MD97-2120 are not included in the deep Indian or deep Pacific age models (Figures 2b and 2c).

The four regional Atlantic age models were similarly developed, except that we used MD95-2042 on the Greenland Ice Core Chronology 2005 (GICC05) age model [*Svensson et al*., 2008; *Stern and Lisiecki*, 2013] as the alignment target (Figures 2d–2g). Instead of averaging the available age estimates every 10 cm on the MD97-2120 depth scale, we averaged age estimates across all available cores every 500 years on based on their alignment to MD95-2042 on the GICC05 age model. We emphasize here that the MD95-2042/GICC05 age model only represents an intermediate step in the construction of our regional Atlantic age models, effectively providing a set of aligned depths that are more evenly spaced in time for creating the various Atlantic age models. Final regional age models are based only on the average of radiocarbon age estimates from the cores in each region (e.g., MD95-2042 ^{14}C ages are only included in the deep North Atlantic age model) and the GICC05 age estimates are not included in our radiocarbon age models.

Monte Carlo samples ($n = 10{,}000$) of age estimates for each core were generated by Bacon and propagated through our entire regional age model generation procedure to provide robust 95% confidence intervals for our age models (Table S2 in the supporting information) assuming constant reservoir ages. These uncertainty estimates implicitly include the effects of any errors in benthic δ^{18}O alignment because alignment errors would increase scatter in the radiocarbon compilations (by aligning portions of cores with different ages) and, thus, increase our age uncertainty estimates. Because our uncertainty estimates do not include possible reservoir age changes, we do not use dates from Atlantic cores located north of 40°N where large-scale reservoir age changes are likely [*Stern and Lisiecki*, 2013]. The evidence for and possible effects of reservoir age changes in other regions are discussed in section 4.3.

2.3. Benthic δ^{18}O Stacking

Benthic δ^{18}O data were stacked (averaged) after a three-step alignment and age conversion process. First, Match was used to align each δ^{18}O record to a target. Indian and Pacific records were aligned to MD97-2120

Table 1. Regional Benthic δ^{18}O Stacks Summary[a]

Region	Number of Cores	Number of Dated Cores	Number of Dates	Resolution (kyr)	Mean Number of δ^{18}O Data per Interval
INA	20	4	42	0.5, sm	47
DNA	94	14	223	0.5	73
ISA	8	4	41	0.5, sm	9
DSA	35	6	123	0.5, sm	38
IP	20	14	160	0.5, sm	31
DP	64	15	194	0.5	34
DI	11	4	69	0.5, sm	21

[a]INA = intermediate North Atlantic, DNA = deep North Atlantic, ISA = intermediate South Atlantic, DSA = deep South Atlantic, IP = intermediate Pacific, DP = deep Pacific, DI = deep Indian, and sm = smoothed using a 1 kyr window (see text).

δ^{18}O versus depth; Atlantic records were aligned to MD95-2042 δ^{18}O on the GICC05 age model. To ensure well-constrained alignments, nearly all of our δ^{18}O records (95%) have an average resolution better than 3000 years. Second, we used the regional radiocarbon age models (Figure 2) to convert each individual record from target depth (or GICC05 age) to its final regional radiocarbon age. Third, we created the stacks by averaging δ^{18}O data placed on the radiocarbon age models.

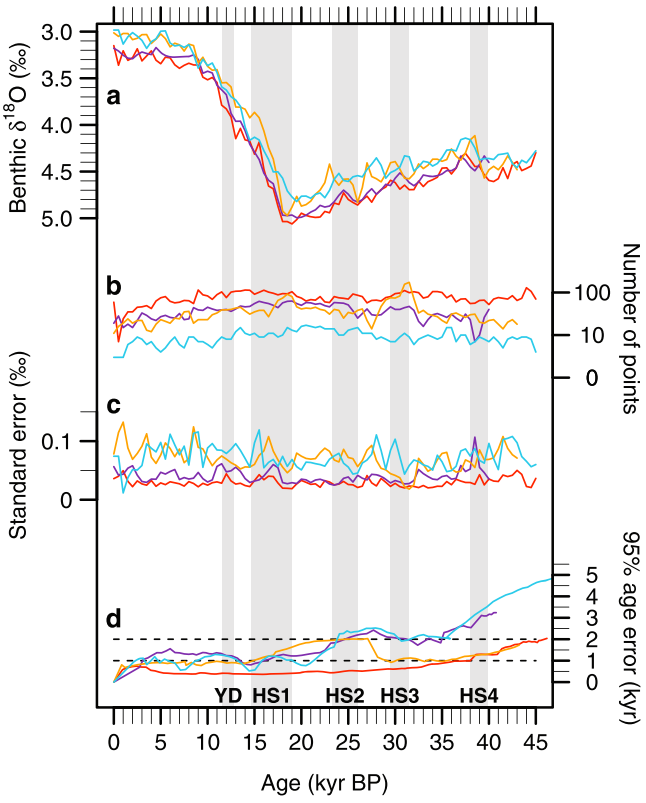

Figure 3. Statistics related to regional stacks of the Intermediate North Atlantic (orange), deep North Atlantic (red), intermediate South Atlantic (light blue), and deep South Atlantic (purple). (a) Regional benthic δ^{18}O stacks, (b) numbers of points per stacked interval (note logarithmic scale), (c) stacked δ^{18}O standard errors, and (d) the length of the 95% age confidence interval. Dashed horizontal lines mark 1 and 2 kyr age error for reference. Age uncertainties are asymmetric—see Table S2 for upper and lower 95% limits. Stacked benthic δ^{18}O values and their standard errors are available in Table S4. All data are plotted relative to our regional radiocarbon age models. Vertical gray bars mark the Younger Dryas (YD) and Heinrich stadials (HS) 1–4.

Although normalized versions of the benthic δ^{18}O records were used for Match alignments, species-corrected benthic δ^{18}O values were used to generate the stacks. The stacks include δ^{18}O data from 17 different genera of benthic foraminifera, but over 90% of the records are from *Cibicidoides* and/or *Uvigerina* species (Table S1 in the supporting information). We used species-correction factors from the original publication of the records where available or applied widely accepted values (Table S3). We follow the conventional assumption that *Uvigerina* spp. δ^{18}O calcify in equilibrium with surrounding seawater [*Shackleton*, 1974; *Fontanier et al.*, 2006], but a few studies suggest that *Cibicidoides* species may record equilibrium conditions at some Pacific sites [*Ohkushi et al.*, 2003; *Nürnberg et al.*, 2004; *Herguera et al.*, 2010]. Although a few benthic foraminiferal species may have time-dependent δ^{18}O offsets [*Hoogakker et al.*, 2010], we do not include data from these species in our stacks.

We stacked the δ^{18}O records by averaging all available benthic δ^{18}O values within evenly spaced time intervals on the regional ^{14}C age models. Because we average individual measurements within each interval (instead of using interpolated values), high-resolution records have a greater influence on the

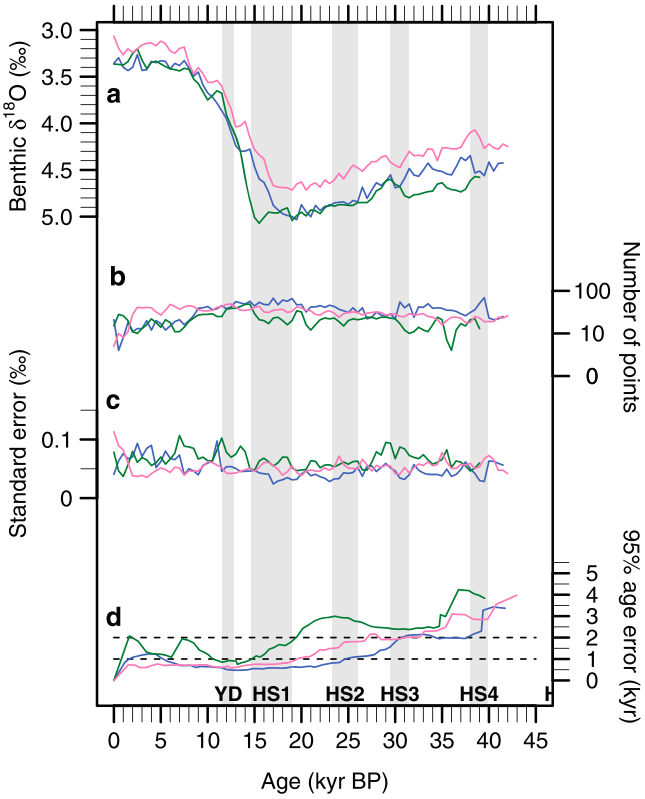

Figure 4. Statistics related to regional stacks of the deep Pacific (blue), deep Indian (green), and intermediate Pacific (pink). (a–d) Same as Figure 3.

stacks than low-resolution records. In the deep North Atlantic and deep Pacific regions, stack δ^{18}O values are calculated every 500 years by averaging all available benthic δ^{18}O values within ±250 years on the regional ^{14}C age model. In the other regions with fewer available cores, stack δ^{18}O values are calculated every 500 year by averaging all available benthic δ^{18}O values within ±500 years. These overlapping bins smooth the stacks while still allowing for convenient comparison with higher-resolution records. Table 1 summarizes the number of cores, ^{14}C dates, and δ^{18}O observations included in each stack. Regional ^{14}C age model uncertainties and standard errors for stacked δ^{18}O values are reported in Figures 3 and 4 and Tables S2 and S4 in the supporting information.

3. Results

3.1. Overview

The seven regional stacks are generally similar over the last 40 kyr, except that the timing of the last deglacial decrease in benthic δ^{18}O varies by up to 4000 years and the intermediate stacks are shifted to lighter δ^{18}O values than the deep stacks. All the stacks exhibit long-term increases from about 40 to 20 kyr B.P. with superimposed millennial-scale variability during the glacial period; prominent millennial-scale decreases occur during Heinrich stadials and at ~36.5 and ~27.5 kyr B.P. (Figures 3 and 4). However, we refrain from interpreting these millennial-scale features because age model uncertainties are larger during the glacial period (95% confidence interval (CI) generally around ±1000–2000 years) and these small magnitude events are not reproducible for different sets of alignments (section 4.1).

The Last Glacial Maximum (LGM), which is defined as 19–26 kyr B.P. based on sea level and ice volume reconstructions [*Clark et al.*, 2009], begins significantly before maximum benthic δ^{18}O. Maximum δ^{18}O values in most of the regional stacks occur at the end of the LGM, between 18.5 and 19.5 kyr B.P. (Table 2). Deglacial benthic δ^{18}O decrease in these regions begins 500–2500 years after the start of sea level rise at 19 kyr B.P. However, a significantly later response is observed in the deep Indian stack, which does not reach its δ^{18}O maximum until 15.5 (15.0–16.1) kyr B.P.

Table 2. Termination Onset Ages (in kiloyears B.P.)[a]

Region	Age of Maximum δ^{18}O	Termination Onset Age	Termination Onset Age Lower 95% Limit	Termination Onset Age Upper 95% Limit
INA	18.5	17.5	16.8	18.2
DNA	19.0	17.5	17.3	17.7
ISA	19.5	18.5	17.9	19.0
DSA	19.5	17.5	16.9	18.1
IP	19.0	16.5	16.1	16.9
DP	19.5	17.5	17.2	17.8
DI	15.5	14.5	14.1	15.0

[a]Abbreviations as in Table 2.

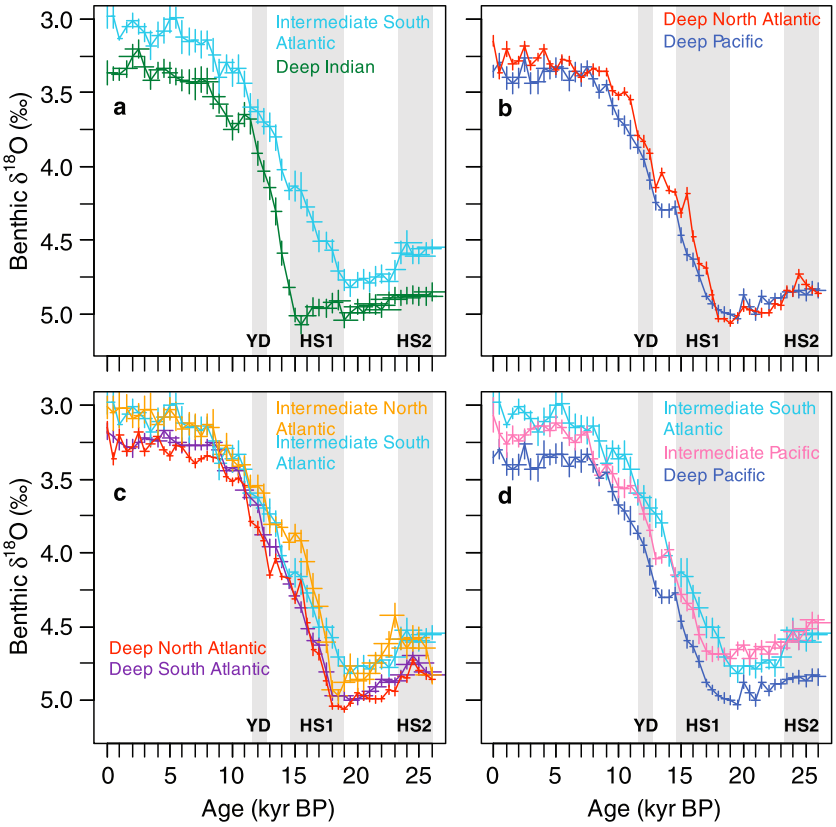

Figure 5. Regional benthic δ^{18}O stacks comparisons for Termination 1. Error bars show the 95% age uncertainty and ±1 standard error for stacked δ^{18}O values.

Glacial-interglacial δ^{18}O changes in the stacks (maximum-minimum values) range from 1.65 to 1.96‰ (for the Intermediate Pacific and Intermediate North Atlantic, respectively). Although regional differences in the magnitude of glacial-interglacial change are not statistically significant, we do observe a systematic pattern. The two North Atlantic stacks have the largest glacial-interglacial changes, the South Atlantic and Indian stacks have intermediate changes, and the two Pacific stacks have the smallest changes.

We choose not to analyze regional δ^{18}O gradients because of several uncertainties. First, temporal changes in the gradient between two stacks could be caused either by changing the dominant water mass properties in one or both regions or by shifting water mass boundaries. Second, the stacked δ^{18}O values could be biased by the depth distribution of cores within each region, with shallower cores generally contributing lighter δ^{18}O. Third, different species of benthic foraminifera dominate different regions of the deep ocean. Atlantic stacks contain proportionately more data from *Cibicidoides* species than *Uvigerina* species compared to the Pacific stacks (Table S1 in the supporting information), although species offset corrections should compensate for this (section 2.3). Fourth, interlaboratory calibration differences can cause offsets up to ~0.3‰ in measured δ^{18}O [*Ostermann and Curry*, 2000]; however, the effect on our stacks should be minor due to the large number of cores used.

3.2. Termination 1 Timing

By defining the termination onset as the first stacked δ^{18}O point that is at least 0.1‰ lighter than the maximum δ^{18}O value (Table 2), we identify a 4000 year difference between the earliest termination onset at 18.5 (95% CI: 17.9–19.0) kyr B.P. in the intermediate South Atlantic and the latest termination onset at 14.5 (14.1–15.0) kyr B.P. in the deep Indian (Figure 5a). The deep Indian termination onset occurred across the transition into the Bølling-Allerød and is corroborated by all four dated records that constrain the deep Indian age model (see discussion in section 4.6). The termination onset occurs at 17.5 kyr B.P. in the deep North

Atlantic (17.3–17.7 kyr B.P.), deep South Atlantic (16.9–18.1 kyr B.P.), deep Pacific (17.2–17.8 kyr B.P.), and intermediate North Atlantic (16.8–18.2 kyr B.P.). The intermediate Pacific termination onset occurs at 16.5 (16.1–16.9) kyr B.P., significantly later than both the intermediate South Atlantic (18.5 kyr B.P.) and deep Pacific (17.5 kyr B.P.) (Figure 5d).

Although the deep Atlantic and deep Pacific stack both have termination onsets at 17.5 kyr B.P., a deep Pacific lag compared to the deep North Atlantic is evident in the middle of the termination (Figure 5b). We estimated the average deep Pacific lag relative to the deep North Atlantic during the termination using two techniques. First, we compared the sum of squared differences over the termination (17.5 to 7.5 kyr B.P.) between the two stacks using their original age models and then shifting the deep Pacific stack older by 0–4000 years in increments of 500 years. The minimum sum of squared differences (i.e., the best agreement between the stacks) occurred when the deep Pacific stack was shifted 1000 years older. This result is not sensitive to small changes in the age window used to define the termination. Next, we calculated the age difference between the stacks at even 0.1‰ increments by interpolating along the two age models. The deep North Atlantic and deep Pacific stacks have similar δ^{18}O values of 4.90 ± 0.03‰ at 17.5 kyr B.P. and 3.34 ± 0.02‰ at 7.5 kyr B.P., so this technique gives us fifteen age differences for δ^{18}O values between 4.8 and 3.4‰. Where two age differences were possible for a single δ^{18}O value because of a δ^{18}O reversal in one of the stacks, we used the smaller age difference in our calculation of the average. The average of these age differences is 800 years, with a maximum age difference of 1700 years occurring at 4.2‰, in the middle of the termination. We conclude that deep Pacific benthic δ^{18}O lagged deep North Atlantic benthic δ^{18}O by an average of ~1000 years during the termination, with a maximum lag of 1700 years during the middle of the termination.

4. Discussion

4.1. Sensitivity to Alignment Target

We test the robustness of our stacks and age models by making different versions of the intermediate North and South Atlantic stacks using different alignment targets (particularly selecting cores from within each region to use as targets). Our primary set of alignments use MD95-2042 (from 3146 m on the Iberian Margin) as the Atlantic target core and MD97-2120 (from 1210 m near New Zealand) as the Indian and Pacific target core. We made two additional intermediate North Atlantic stacks with different alignment targets, Ocean Drilling Program (ODP)983 [*Channell et al*., 1997; *Raymo et al*., 2004] and M35003-4 [*Rühlemann et al*., 2004] on their own depth scales. Similarly, we made an additional intermediate South Atlantic stack using GeoB1711 [*Little et al*., 1997; *Vidal et al*., 1999] as the target. In all stacks for a given region, the timing of early deglacial features, including termination onsets, is consistent regardless of alignment target (Figure S2 in the supporting information). Therefore, we conclude that termination onset ages are not biased by choice of alignment target, including the use of targets from outside that region (e.g., intermediate North Atlantic records aligned to MD95-2042, a deep North Atlantic target).

Glacial millennial-scale features, however, do appear to be sensitive to the choice of target core. All versions of the intermediate North and South Atlantic stacks exhibit some millennial-scale variability during the glacial period, but most of these features are not reproducible (Figure S2 in the supporting information). Some of the differences are likely due to the influence of the target core itself, with each stack tending to reproduce the millennial-scale features present in its alignment target. Because two different targets from within the same region (ODP983 and M35003-4) produce different millennial-scale features, we could not confidently interpret these features even if each regional stack used an alignment target from within that region. Instead, using one Atlantic and one Indo-Pacific target allows future studies to redefine region boundaries without having to realign cores to different regional targets. Lastly, we caution that millennial-scale features are not well-defined in many cores; thus, their alignment is somewhat subjective and may differ between researchers even if the same alignment target were used. In contrast, alignment of the glacial termination is less subjective and more easily reproducible.

4.2. Benthic δ^{18}O Synchrony Within Regions

To construct our regional age models, we assumed that benthic δ^{18}O changes are synchronous within each of the seven regions. Several modeling studies suggest that this assumption is usually valid to within a few hundred years [*Wunsch and Heimbach*, 2008; *Ganopolski and Roche*, 2009; *Primeau and Deleersnijder*, 2009;

Siberlin and Wunsch, 2011; *Friedrich and Timmermann*, 2012], which is smaller than the resolution of the stacks and within their reported age model uncertainties. However, some intraregional differences do exist with respect to benthic δ^{18}O features (e.g., amplitudes of change and termination reversals) and perhaps the timing of δ^{18}O changes. For example, some intermediate North Atlantic cores show δ^{18}O reversals during HS1 while others do not, and some North Atlantic cores from 2000 to 2500 m differ from those below 2500 m [*Schonfeld et al*., 2003; *Labeyrie et al*., 2005; *Waelbroeck et al*., 2011]. Despite some level of variability within each region, the regional stacks can be used to evaluate the average properties of δ^{18}O change within each region. Any diachronous δ^{18}O change in ^{14}C-dated cores from within a region will create scatter within the regional ^{14}C age model (Figure 2) and hence widen the age model uncertainty.

However, because some areas within the regions have relatively sparse coverage, the timing of change within these areas is less well constrained. Most notably, the relatively small number of dated cores from the South Pacific limits our ability to evaluate variability in the timing of δ^{18}O response within the intermediate and deep Pacific. Although modeling experiments suggest a South Pacific lead over North Pacific benthic δ^{18}O during the termination [e.g., *Wunsch and Heimbach*, 2008; *Friedrich and Timmermann*, 2012], we are unable to create four separate Pacific regional stacks due to the scarcity of ^{14}C-dated Pacific cores. Therefore, extra caution should be used when comparing the relative timing of changes between the North and South Pacific using our Pacific age models.

4.3. Marine ^{14}C Reservoir Ages

A reservoir age is the difference between the radiocarbon age of the surface ocean and the contemporaneous atmosphere and is required for calibrating marine radiocarbon ages to calendar ages. Careful consideration of reservoir ages is critical to our study because past reservoir ages may have varied by $>$1000 ^{14}C yr at particular locations (see below) and reservoir ages are spatially correlated. The modern (prebomb) global mean reservoir age is 405 ^{14}C yr [*Reimer et al*., 2013], and modern reservoir ages at the sites used in our compilation range from about 300 to 900 ^{14}C yr. We use constant 405 ^{14}C yr reservoir ages throughout this study.

4.3.1. Atlantic Reservoir Ages

Because regionally averaged high-latitude North Atlantic reservoir ages increased to $>$1000 ^{14}C yr from 18.5 to 16.5 kyr B.P. and 900–1000 ^{14}C yr during the Younger Dryas [*Stern and Lisiecki*, 2013], the North Atlantic age models presented in this study are based only on dates from cores located south of 40°N. Low-latitude North Atlantic reservoir ages probably remained within a couple hundred years of the modern average, and the same is likely true of the low-latitude South Atlantic (see discussion in *Stern and Lisiecki* [2013]). Our intermediate South Atlantic age model is constrained by dates from four cores located between 20 and 30°S, but the deep South Atlantic age model includes cores from as far south as 44°S.

In the high-latitude South Atlantic, *Skinner et al*. [2010] reported increased surface reservoir ages from 23 to 16.5 kyr B.P. and around 13.2 kyr B.P. for MD07-3076 (44°S), with peak reservoir ages $>$2000 ^{14}C yr during the early deglaciation. We use a constant 405 ^{14}C yr reservoir age for this site in our deep South Atlantic age model, but excluding dates from this core or using *Skinner et al*.'s [2010] increased reservoir ages only shifts the deep South Atlantic stack by a maximum of 100–200 years younger during the termination (and has no effect on the termination onset timing). The effect of excluding or shifting the age model of this single core is small on our regionally averaged age model because our deep South Atlantic age model represents the average of age estimates from 5 to 6 dated cores over the termination.

Skinner et al. [2010] argue for constant reservoir ages at 41°S in the South Atlantic, suggesting that the reservoir age increases recorded in MD07-3076 may be a local phenomenon (or, at least, limited to $\geq$44°S). Previous studies use constant reservoir ages between 400 and 800 ^{14}C yr for the cores from 41 to 43°S that are included in our deep South Atlantic age model [*Becquey and Gersonde*, 2003; *Piotrowski et al*., 2004; *Molyneux et al*., 2007]. *Molyneux et al*. [2007] allow for the possibility that reservoir ages may have been up to 1800 ^{14}C yr at MD02-2589 based on aligning benthic δ^{18}O to intermediate Pacific site MD97-2120 [*Pahnke et al*., 2003]. However, our stacks indicate that diachronous benthic δ^{18}O responses between the deep South Atlantic and intermediate Pacific offer an alternative explanation to the proposed South Atlantic reservoir age changes, and we note that past reservoir ages near New Zealand are also the subject of debate.

4.3.2. Pacific Reservoir Ages

Reservoir age estimates near New Zealand have been estimated by comparing terrestrial and planktonic foraminiferal ^{14}C dates from near six tephra layers [*Sikes et al*., 2000]. Reservoir ages were estimated to be ~400–500 ^{14}C yr for most of the interval from 0 to 17.5 kyr B.P., 800 ^{14}C yr in the middle of the Bølling-Allerød, and ~2000 ^{14}C yr during the Kawakawa Ash (27.1 kyr B.P. ± 1 kyr) [*Lowe et al*., 2008]. *Pahnke et al*. [2003] originally assumed constant reservoir ages for core MD97-2120, also from near New Zealand, but later updated their age model for this core using the *Sikes et al*. [2000] reservoir ages [*Pahnke and Zahn*, 2005]. However, *Carter et al*. [2008] found no evidence for an exceptionally large reservoir age at the time of the Kawakawa Ash in another nearby New Zealand core, showing that the magnitude and extent of this possible ~27 kyr B.P. reservoir age increase is still very uncertain.

Using Bacon and constant 405 ^{14}C yr reservoir ages, we calculate an age of 23.1 (20.3–28.2) kyr B.P. for the Kawakawa Ash in MD97-2120 using only that core's dates, or 25.5 (23.9–27.0) kyr B.P. using our intermediate Pacific age model. The age of the ash in the CHAT1K core (which does not have radiocarbon dates) on the deep Pacific age model is 26.4 (25.3–27.4) kyr B.P. Thus, there is reasonable agreement between the age of the Kawakawa Ash in MD97-2120 and CHAT1K on our age models and the estimate of 27.1 kyr B.P. ± 1 kyr [*Lowe et al*., 2008]. Allowing for a ~2000 ^{14}C yr reservoir age at MD97-2120 would make our ash age estimates even younger and significantly worsen this agreement, suggesting that this reservoir age increase is unlikely.

Data from *Sikes et al*. [2000] and *Carter et al*. [2008] support reservoir ages of 600–800 ^{14}C yr near New Zealand from the middle of the Bølling-Allerød (BA) into the Younger Dryas (YD). Our ages for MD97-2120 and Deep Sea Drilling Project 540 (both from the Chatham Rise) are indeed older than the average intermediate Pacific age model during this interval, while our ages from H214 (Bay of Plenty) are slightly younger than the average deep Pacific age model at this time. Thus, our results are consistent with a small reservoir age increase during the BA/YD near New Zealand but suggest that this increase was probably restricted to southern sites. However, this small change in BA/YD reservoir ages near southern New Zealand is within the uncertainty of our age models and not significant given the resolution of our stacks.

Reservoir ages between 1000 and 1700 ^{14}C yr have been observed during the first half of the deglaciation in MD01-2416 and MD02-2489 from the high-latitude (>50°N) North Pacific [*Sarnthein et al*., 2007; *Gebhardt et al*., 2008]. Additionally, in the northern South China Sea, *Sarnthein et al*. [2007] reconstructed reservoir ages up to ~2000 ^{14}C yr during the LGM and early deglaciation in core GIK17940. However, these three Pacific cores do not show any significant deviations from our mean age models in the intervals where increased reservoir ages have been proposed. Thus, excluding dates from these sites would have a negligible effect on our age model. These results could be consistent with either (1) relatively small reservoir age changes at these sites, (2) diachronous δ^{18}O change that is disguised by reservoir age change, or (3) pervasive reservoir age changes throughout the Pacific.

4.3.3. Summary

In summary, possible past reservoir age variability is probably least problematic for our intermediate North Atlantic, deep North Atlantic, and intermediate South Atlantic age models, where all the dated records are from <40° latitude and reservoir ages likely remained within a couple hundred years of modern. The deep South Atlantic age model is less certain because it contains ages from higher latitude sites. Even a ~2000 ^{14}C yr reservoir age increase at MD07-3076 would have only a minor effect on our deep South Atlantic age model, but similarly large reservoir ages throughout the high-latitude (e.g., >40°S) South Atlantic would shift the stack up to ~1000 years younger. The effect of increasing reservoir ages in the Pacific or Indian would be to shift those age models younger, increasing the Pacific lag relative to the Atlantic or making the deep Indian termination onset even later.

4.4. Intermediate Atlantic Termination Responses

The termination onset in our intermediate North Atlantic stack is 17.5 (16.8–18.3) kyr B.P. and has a relatively wide 95% confidence interval that overlaps with the intermediate South Atlantic at 18.5 (17.9–19.0) kyr B.P. However, our estimated age of 17.5 kyr B.P. for the intermediate North Atlantic termination onset is in good agreement with previous compilations [*Sarnthein et al*., 1994; *Waelbroeck et al*., 2011], and several lines of evidence suggest that the intermediate North Atlantic onset occurred no earlier than 17.5 kyr B.P. The well-dated intermediate North Atlantic core M35003-4 (12°N), which is included in our age model calculation,

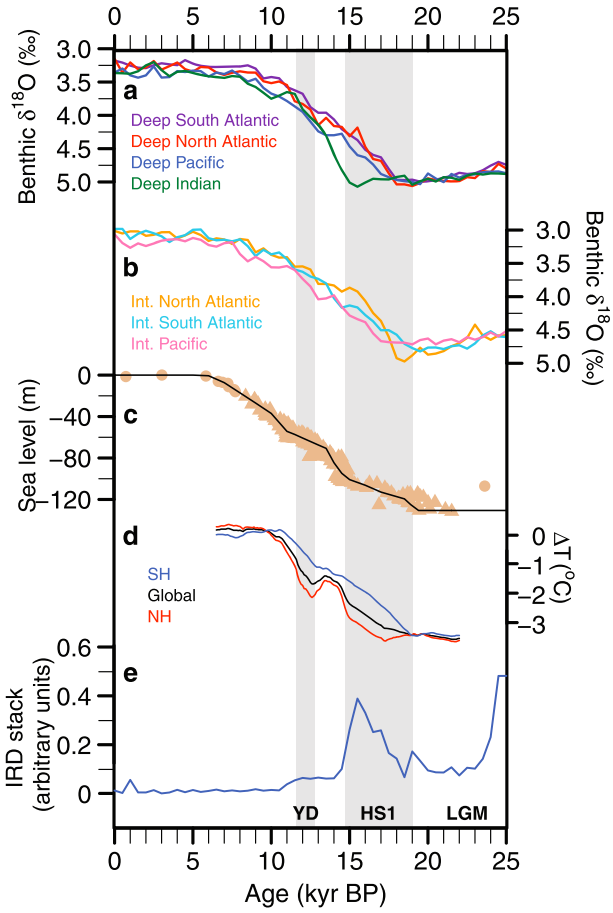

Figure 6. Regional benthic δ^{18}O stacks compared with other climate proxies for the last deglaciation. (a) Deep stacks. (b) Intermediate stacks. (c) Triangles show adjusted sea level data from Sunda Shelf, Tahiti, Barbados, Bonaparte Gulf, and New Guinea for the deglaciation [*Bassett et al.*, 2005; *Clark et al.*, 2012; *Carlson and Clark*, 2012, and references therein]. Global eustatic line [*Bassett et al.*, 2005; *Clark et al.*, 2009, 2012; *Carlson and Clark*, 2012]. Circles show sea level data from [*Bard et al.*, 1996; *Cutler et al.*, 2003; *Peltier and Fairbanks*, 2006]. (d) Temperature stacks: global (black), northern hemisphere (red), and southern hemisphere (blue) [*Shakun et al.*, 2012]. (e) Ice-rafted debris (IRD) stack [*Stern and Lisiecki*, 2013].

shows a clear termination onset at 17.5 kyr B.P. [*Rühlemann et al.*, 1999, *Rühlemann et al.*, 2004; *Hüls and Zahn*, 2000]. Two radiocarbon dates near the termination onset in another core from the stack (PO200-10-6-2, 38°N) also corroborate this timing [*Baas et al.*, 1997].

The age of the intermediate North Atlantic termination onset can also be constrained by comparing the phase of benthic δ^{18}O relative to ice-rafted debris (IRD) in individual cores. The stratigraphy and timing of North Atlantic IRD deposits during the beginning of the last deglaciation are well known, with so-called precursor IRD beginning around 18 kyr B.P., an initial IRD peak at 17 kyr B.P. (termed Heinrich Event 1), and a later, larger IRD peak at 16 kyr B.P. [e.g., *Stern and Lisiecki*, 2013]. In intermediate North Atlantic cores with both benthic δ^{18}O and IRD, the termination onset consistently occurs near the same depth as an IRD peak [*Venz et al.*, 1999; *Van Kreveld et al.*, 2000; *Thornalley et al.*, 2010], thus suggesting termination onsets between around 16.0 and 17.5 kyr B.P. However, because these sites are all from high latitudes (55–65°N), they are not included in the intermediate North Atlantic age model due to likely reservoir ages changes. For example, *Thornalley et al.* [2010] place the intermediate North Atlantic termination onset around 16.5 kyr B.P. in three cores taken just south of Iceland from 1200 to 2300 m depth, using age models with ~2000 ^{14}C yr reservoir ages. Similar reservoir ages at SO82-5-2 (59°N) would yield a termination onset age of ~17 kyr B.P. using that core's planktonic ^{14}C dates [*Van Kreveld et al.*, 2000]. A somewhat smaller reservoir age closer to 1000 ^{14}C yr, as suggested by *Stern and Lisiecki* [2013], would shift the termination onset at SO82-5-2 into excellent agreement with our stack's low-latitude age model. Thus, additional constraints from high-latitude radiocarbon ages as well as the relative phase between benthic δ^{18}O and IRD make it unlikely that the intermediate North Atlantic termination onset occurred any earlier than 17.5 kyr B.P.

Waelbroeck et al. [2011] proposed synchronous intermediate North and South Atlantic benthic δ^{18}O termination onsets at 17.5 kyr B.P. associated with Atlantic Meridional Overturning Circulation (AMOC) changes triggered by Heinrich Event 1 melting. However, we find that the intermediate South Atlantic termination onset at 18.5 (17.9–19.0) kyr B.P. significantly preceded peak Heinrich Event 1 ice-rafted debris at 17.0 (16.7–17.3) kyr B.P. [*Stern and Lisiecki*, 2013]. Thus, the initial deglacial benthic δ^{18}O decrease in the intermediate South Atlantic is more likely related to 19 kyr B.P. melting and AMOC change [e.g., *Stern and Lisiecki*, 2013] (Figure 6).

We consider three possible explanations for an early intermediate South Atlantic termination onset: increased low-latitude South Atlantic reservoir ages, the arrival of light δ^{18}O from meltwater, and subsurface warming. As discussed in the previous section, available evidence suggests that reservoir ages around 20–30°S

in the Atlantic probably remained within a few hundred years of modern. To shift the intermediate South Atlantic stack into agreement with the intermediate North Atlantic termination onset age would require reservoir ages of ~1500 ^{14}C yr, which are quite unlikely in the subtropical Atlantic.

Sea level rise at 19 kyr B.P. was 5–10 m and came mostly from Northern Hemisphere ice sheets [*Carlson and Clark*, 2012]. Therefore, if light δ^{18}O from meltwater caused the intermediate South Atlantic termination onset, the termination onset should occur first in the North or synchronously with the South to within uncertainty. Although our reported uncertainties allow for synchronous termination onsets in the intermediate North and South Atlantic, additional stratigraphic constraints provided by IRD and high-latitude ^{14}C dates suggest that the intermediate North Atlantic termination onset likely occurred later. Also, the total amount of meltwater at 19 kyr B.P. would cause seawater δ^{18}O to decrease by less than 0.1‰ globally, and the minor amount of Southern Hemisphere ice sheet melting at this time would probably not register a detectable benthic δ^{18}O decrease. In summary, light δ^{18}O from meltwater was unlikely to be more than a minor contribution to the early intermediate South Atlantic termination onset because Northern Hemisphere melting was not recorded in the intermediate North Atlantic at 19 kyr B.P. and Southern Hemisphere melting was minor.

However, Northern Hemisphere meltwater at 19 kyr B.P. was sufficient to weaken the AMOC and initiate a bipolar seesaw response that caused widespread Southern Hemisphere surface warming beginning at 19 kyr B.P. [*Shakun et al*., 2012]. Therefore, warming was most likely the dominant contributor to the early intermediate South Atlantic termination onset (Figure 6). Southern surface warming might have been transferred to the intermediate South Atlantic through the formation of Antarctic Intermediate Water (AAIW); however, it is currently a matter of debate whether AAIW expanded [*Pahnke et al*., 2008] or contracted [*Xie et al*., 2012] during this interval.

AMOC weakening at 19 kyr B.P. [e.g., *Shakun et al*., 2012; *Stern and Lisiecki*, 2013] may also have caused a bipolar seesaw response in intermediate-depth temperatures. In our stacks an intermediate North Atlantic δ^{18}O increase (cooling) is coeval with the intermediate South Atlantic δ^{18}O decrease (warming) at 18.5–19 kyr B.P. (Figure 5c). However, the magnitude and timing of the 19 kyr B.P. increase in intermediate North Atlantic δ^{18}O is somewhat inconsistent between stacks produced using different alignment targets (Figure S2 in the supporting information). Some model results show a bipolar seesaw temperature response at intermediate depths with reduced AMOC [*Stocker and Johnsen*, 2003], but this is not a consistent feature across all models [*Stocker et al*., 1992, 2007; *Mignot et al*., 2007; *Liu et al*., 2009].

From 18 to 15 kyr B.P. benthic δ^{18}O decreased by 1.09‰ in the intermediate North Atlantic while sea level rose by a maximum of 30 m [*Carlson and Clark*, 2012]. Scaling the glacial-interglacial 130 m sea level rise [*Carlson and Clark*, 2012] to the average seawater δ^{18}O decrease of 1.05‰ [*Adkins et al*., 2002; *Duplessy et al*., 2002] suggests that only about a 0.25‰ global average benthic δ^{18}O decrease over HS1 can be explained by ice volume change. Explanations for the remaining intermediate North Atlantic HS1 benthic δ^{18}O decrease have formed two camps: one emphasizing warming [e.g., *Rühlemann et al*., 2004; *Marcott et al*., 2011] and the other focusing on brine formation [e.g., *Dokken and Jansen*, 1999; *Waelbroeck et al*., 2011]. Distinguishing between these two hypotheses requires independent constraints on water mass properties and/or temperatures. Our intermediate North Atlantic stack could be consistent with warming, brine formation, or a combination of both but provides the constraint that these mechanisms must account for the magnitude of the observed δ^{18}O decrease throughout the intermediate North Atlantic during HS1.

4.5. Pacific Termination Lag

Because the intermediate Pacific termination onset at 16.5 kyr B.P. is significantly later than the intermediate South Atlantic onset at 18.5 kyr B.P., the timing of the initial deglacial benthic δ^{18}O decrease was not globally synchronous at intermediate depths, in contradiction with the hypothesis of *Waelbroeck et al*. [2006, 2011]. *Pahnke et al*. [2008] proposed an early 19 kyr B.P. expansion of Antarctic Intermediate Water in the Atlantic and a later 17 kyr B.P. expansion in the Pacific. This provides one possible explanation for the termination onset occurring much earlier in the intermediate South Atlantic compared to the intermediate Pacific. Model results [*Friedrich and Timmermann*, 2012] suggest another possible explanation. With modern circulation, these authors show that light δ^{18}O entering the surface North Atlantic would propagate into the Pacific at depth and then mix vertically, consistent with our observation of the deglacial δ^{18}O decrease occurring in the deep Pacific before the intermediate Pacific. However, with reduced AMOC, light δ^{18}O entered the intermediate Pacific

before the deep Pacific, partly due to the development of a Pacific meridional overturning circulation. So, while *Friedrich and Timmermann* [2012] suggest top-down propagation of light $\delta^{18}O$ in the Pacific during HS1, our regional stacks seem to suggest bottom-up transport.

Skinner and Shackleton [2005] found a 3900 year age difference in the midpoint of deglacial benthic $\delta^{18}O$ change between MD99-2334 (deep North Atlantic) and TR163-31 (deep eastern equatorial Pacific), which they attributed to delayed Pacific warming. However, we find a 1000 year average and 1700 year maximum termination lag of mean deep Pacific benthic $\delta^{18}O$ behind mean deep Atlantic benthic $\delta^{18}O$. This smaller but still significant lag agrees well with the sedimentation rate analysis of *Lisiecki and Raymo* [2009]. The larger lag estimated by *Skinner and Shackleton* [2005] appears to result from local signals in the cores analyzed. The feature that defines the termination midpoint in *Skinner and Shackleton*'s [2005] deep North Atlantic record occurs at 15 kyr B.P. on their age model but at 16 kyr B.P. in our deep North Atlantic stack. Additionally, the benthic $\delta^{18}O$ decrease during HS1 in *Skinner and Shackleton*'s [2005] deep Pacific core is only about half the amplitude of the deep Pacific stack.

4.6. Deep Indian Termination Timing

The latest termination onset occurs in the deep Indian stack at 14.5 kyr B.P. This late onset cannot be an artifact of surface reservoir age change because increasing Indian reservoir ages would shift the age model even younger while decreasing reservoir ages could shift the stack older by at most ~400 years. Such a late deep Indian termination onset was not predicted by modeling studies that addressed the timing of deglacial benthic $\delta^{18}O$ changes [*Wunsch and Heimbach*, 2008; *Ganopolski and Roche*, 2009; *Primeau and Deleersnijder*, 2009; *Siberlin and Wunsch*, 2011; *Friedrich and Timmermann*, 2012; *Gebbie*, 2012], which suggests that something important is missing from our understanding of HS1 ocean circulation changes and water mass properties.

The late deep Indian benthic $\delta^{18}O$ response could result from slow transport of the deglacial $\delta^{18}O$ signal to the deep Indian Ocean in general or to a specific region within it, as data coverage is sparse. The four dated records from the deep Indian Ocean in our compilation come from a narrow depth range (3200–3300 m), with three cores from between 40 and 50°S and one from the Arabian Sea (Figure 1 and Table S1 in the supporting information). However, a similarly late termination onset was also observed in a slightly deeper core (3420 m) from 40 to 50°S [*Smart et al*., 2010] and at 3800 m near the southern tip of India [*Piotrowski et al*., 2009]. In contrast, a ^{14}C-dated Indian Ocean record from 2100 m shows a much earlier termination onset [*Waelbroeck et al*., 2006]. So, while the spatial extent of the late Indian Ocean termination onset remains uncertain, intermediate depths probably did not experience this extreme delay.

The heavy HS1 $\delta^{18}O$ values in the deep Indian could be caused by regional water mass properties. Glacioeustatic effects are only expected to cause up to a 0.25‰ decrease in global average benthic $\delta^{18}O$ over HS1, so most of the large HS1 decreases in the other regional stacks are due to nonglacioeustatic effects. A 1°C cooling or small salinity increase could mask the glacioeustatic $\delta^{18}O$ decrease in the deep Indian. Very saline waters have been observed during the LGM in the Red Sea [*Siddall et al*., 2003] and deep Southern Ocean [*Adkins et al*., 2002], and *Gebbie* [2012] proposed that the $\delta^{18}O$ of deep water from the Southern Ocean may have increased during HS1. Thus, the influence of a water mass with heavy $\delta^{18}O$ could explain deep Indian benthic $\delta^{18}O$ during HS1.

One interesting possibility is that a relatively late termination onset may occur at 3000–4000 m throughout the Southern Hemisphere. *Ferrari et al*. [2014] propose that most of the deep ocean was isolated from mixing with intermediate-depth water during the LGM and that maximum South Atlantic ventilation ages (2000–3750 years) occurred at middepths [e.g., *Skinner et al*., 2010], sandwiched between younger waters above [*Burke and Robinson*, 2012] and below [*Barker et al*., 2010]. Potentially, middepth southern water remained isolated from mixing with $\delta^{18}O$-depleted meltwater throughout most of HS1 and, therefore, experienced a delayed Termination 1 onset. This hypothesis is currently difficult to test because very few cores with radiocarbon data are available from 3000 to 4000 m in the middle- to high-latitude South Pacific and South Atlantic, and those sites that are available (e.g., MD07-3076, PS2489-2, and RS147-07) may be affected by surface reservoir age changes [e.g., *Skinner et al*., 2010] that would mask the identification of a late termination onset in our study. Therefore, the late deep Indian termination onset may only appear to be unique due to the availability of deep, southerly sites unaffected be surface reservoir change. Extra caution should be used when applying our deep South Atlantic and Pacific regional age models to sites from 3000 to 4000 m.

Alternatively, 3000–4000 m in the Indian Ocean may truly be the last place to mix with deglacial meltwater if the deep South Atlantic and deep South Pacific were ventilated more rapidly due to moderate mixing with northern intermediate water and possibly some deep water from the North Atlantic and North Pacific [e.g., *Rae et al.*, 2014]. Better mapping the geographic extent of this late termination onset will require well-dated benthic δ^{18}O records from the Indian Ocean, South Pacific, and South Atlantic. Radiocarbon age models for sites north of 40°S would be particularly helpful to reduce the chance of reservoir age changes.

5. Conclusions

Regional δ^{18}O stacks with independent radiocarbon age models allow for more precise age control than correlation to a global stack and could be used by data compilation studies to allow for inclusion of cores which lack radiocarbon dating. Regional stacks also provide valuable targets for modeling efforts to understand deep water temperature changes and δ^{18}O transport during the last deglaciation.

In our radiocarbon-dated regional benthic δ^{18}O stacks, most regions experience δ^{18}O maxima at the end of the LGM between 18.5 and 19.5 kyr B.P. while ages for the onset of Termination 1 vary by up to 4000 year (Table 2). The earliest termination onset occurs in the intermediate South Atlantic at 18.5 kyr B.P., shortly after initial deglacial ice sheet melting at 19 kyr B.P. We find synchronous termination onsets in the deep North Atlantic, deep South Atlantic, and deep Pacific at 17.5 kyr B.P. However, the deep Pacific lags the deep North Atlantic by an average of ~1000 years during the termination, with a maximum lag of 1700 year in the middle of the termination. The intermediate Pacific termination onset occurs at 16.5 kyr B.P., significantly later than both the intermediate South Atlantic and deep Pacific. Most surprisingly, we find that the deep Indian stack has an extremely late δ^{18}O maximum (15.5 kyr B.P.), and its termination onset at 14.5 kyr B.P. is coincident with the transition into the Bølling-Allerød. The possibility exists that this late termination onset may also occur at 3000–4000 m in the South Atlantic and South Pacific.

Acknowledgments

We thank everyone who generated and made available the data used in this study. Funding for this research was provided by NSF grants CMG-1025444 and MGG-0926735. We also thank J. Rae, A. Burke, J. Adkins, and L. Skinner for useful discussions. Regional stack data are available in the supporting information.

References

Adkins, J. F., K. McIntyre, and D. P. Schrag (2002), The salinity, temperature, and δ^{18}O of the glacial deep ocean, *Science*, *298*, 1769–1773.

Bard, E., B. Hamelin, M. Arnold, L. Montaggioni, G. Cabioch, G. Faure, and F. Rougerie (1996), Deglacial sea-level record from Tahiti corals and the timing of global meltwater discharge, Nature, *382*, 241–244, doi:10.1038/38224la0.

Barker, S., G. Knorr, M. J. Vautravers, P. Diaz, and L. C. Skinner (2010), Extreme deepening of the Atlantic overturning circulation during deglaciation, *Nat. Geosci.*, *3*, 567–571.

Baas, J. H., J. Mienert, F. Abrantes, and M. A. Prins (1997), Late Quaternary sedimentation on the Portugese continental margin: Climate-related processes and products, *Palaeogeogr. Palaeoclimatol. Palaeoecol.*, *130*, 1–23.

Bassett, S. E., G. A. Milne, J. X. Mitrovica, and P. U. Clark (2005), Ice sheet and solid Earth influences on far-field sea-level histories, *Science*, *309*, 925–928, doi:10.1126/science.1111575.

Bassinot, F. C., et al. (1994), The astronomical theory of climate and the age of the Brunhes-Matuyama magnetic reversal, *Earth Planet. Sci. Lett.*, *126*, 91–108.

Becquey, S., and R. Gersonde (2003), A 0.55-Ma paleotemperature record from the Subantarctic zone: Implications for Antarctic Circumpolar Current development, *Paleoceanography*, *18*(1), 1014, doi:10.1029/2000PA000576.

Blaauw, M., and J. A. Christen (2011), Flexible paleoclimate age-depth models using an autoregressive gamma process, *Bayesian Anal.*, *6*, 457–474.

Burke, A., and L. F. Robinson (2012), The Southern Ocean's role in carbon exchange during the last deglaciation, *Science*, *335*, 557–561.

Carlson, A. E., and P. U. Clark (2012), Ice sheet sources of sea level rise and freshwater discharge during the last deglaciation, *Rev. Geophys.*, *50*, RG4007, doi:10.1029/2011RG000371.

Carter, L., B. Manighetti, G. Ganssen, and L. Northcote (2008), Southwest Pacific modulation of abrupt climate change during the Antarctic Cold Reversal-Younger Dryas, *Palaeogeogr. Palaeoclimatol. Palaeoecol.*, *260*, 284–298.

Channell, J. E. T., D. A. Hodell, and B. Lehman (1997), Relative geomagnetic paleointensity and δ^{18}O at ODP Site 983 (Gardar Drift, North Atlantic) since 350 ka, *Earth Planet. Sci. Lett.*, *153*, 103–118.

Clark, P. U., et al. (2009), The Last Glacial Maximum, *Science*, *325*, 710–714, doi:10.1126/science.1172873.

Clark, P. U., et al. (2012), Global climate evolution during the last deglaciation, *Proc. Natl. Acad. Sci. U.S.A.*, *109*(19), 1134–1142, doi:10.1073/pnas.1116619109.

CLIMAP Project Members (1981), *Seasonal Reconstructions of the Earth's Surface at the Last Glacial Maximum*, Map Chart Ser. MC-36, Geol. Soc. Am., Boulder, Colo.

Cramer, B. S., J. R. Toggweiler, J. D. Wright, M. E. Katz, and K. G. Miller (2009), Ocean overturning since the Late Cretaceous: Inferences from a new benthic foraminiferal isotope compilation, *Paleoceanography*, *24*, PA4216, doi:10.1029/2008PA001683.

Curry, W. B., and D. W. Oppo (2005), Glacial water mass geometry and the distribution of δ^{13}C of ΣCO_2 in the western Atlantic Ocean, *Paleoceanography*, *20*, PA1017, doi:10.1029/2004PA001021.

Cutler, K. B., et al. (2003), Rapid sea-level fall and deep-ocean temperature change since the last interglacial period, *Earth Planet. Sci. Lett.*, *206*, 253–271.

Dokken, T. M., and E. Jansen (1999), Rapid changes in the mechanism of ocean convection during the last glacial period, *Nature*, *401*, 458–461.

Duplessy, J.-C., L. Labeyrie, and C. Waelbroeck (2002), Constraints on the ocean oxygen isotopic enrichment between the Last Glacial maximum and the Holocene: Paleoceanographic implications, *Quat. Sci. Rev.*, *21*, 315–330.

Ferrari, R., M. F. Jansen, J. F. Adkins, A. Burke, A. L. Sewart, and A. F. Thompson (2014), Antarctic sea ice control on ocean circulation in present and glacial climates, *Proc. Natl. Acad. Sci. U.S.A.*, *111*, 8753–8758.

Fontanier, C., A. Mackensen, F. J. Jorissen, P. Anschutz, L. Licari, and C. Griveaud (2006), Stable oxygen and carbon isotopes of live benthic foraminifera from the Bay of Biscay: Microhabitat impact and seasonal variability, *Mar. Micropaleontol.*, *58*, 159–183.

Friedrich, T., and A. Timmermann (2012), Millennial-scale glacial meltwater pulses and their effect on the spatiotemporal benthic δ^{18}O variability, *Paleoceanography*, *27*, PA3215, doi:10.1029/2012PA002330.

Ganopolski, A., and D. M. Roche (2009), On the nature of lead-lag relationships during glacial-interglacial climate transitions, *Quat. Sci. Rev.*, *28*, 3361–3378.

Gebbie, G. (2012), Tracer transport timescales and the observed Atlantic-Pacific lag in the timing of the Last Termination, *Paleoceanography*, *27*, PA3225, doi:10.1029/2011PA002273.

Gebhardt, H., M. Sarnthein, P. M. Grootes, T. Kiefer, H. Kuehn, F. Schmieder, and U. Röhl (2008), Paleonutrient and productivity records from the subarctic North Pacific for Pleistocene glacial terminations I to V, *Paleoceanography*, *23*, PA4212, doi:10.1029/2007PA001513.

Herguera, J. C., T. Herbert, M. Kashgarian, and C. Charles (2010), Intermediate and deep water mass distribution in the Pacific during the Last Glacial Maximum inferred from oxygen and carbon stable isotopes, *Quat. Sci. Rev.*, *29*, 1228–1245.

Hoogakker, B., H. Elderfield, K. Oliver, and S. Crowhurst (2010), Benthic foraminiferal oxygen isotope offsets over the last glacial-interglacial cycle, *Paleoceanography*, *25*, PA4229, doi:10.1029/2009PA001870.

Hüls, M., and R. Zahn (2000), Millennial-scale sea surface temperature variability in the western tropical North Atlantic from planktonic foraminiferal census counts, *Paleoceanography*, *15*, 659–678.

Imbrie, J., J. D. Hays, D. G. Martinson, A. McIntyre, A. C. Mix, J. J. Morley, N. G. Pisias, W. L. Prell, and N. J. Shackleton (1984), The orbital theory of Pleistocene climate: Support from a revised chronology of the marine δ^{18}O record, in *Milankovitch and Climate, Part 1*, edited by A. Berger, pp. 269–305, Springer, New York.

Kallel, N., L. D. Labeyrie, A. Julliet-Leclerc, and J.-C. Duplessy (1988), A deep hydrological front between intermediate and deep-water masses in the glacial Indian Ocean, *Nature*, *333*, 651–655.

Labeyrie, L. D., J.-C. Duplessy, and P. L. Blanc (1987), Variations in mode of formation and temperature of oceanic deep waters over the past 125,000 years, *Nature*, *327*, 477–482.

Labeyrie, L., C. Waelbroeck, E. Cortijo, E. Michel, and J.-C. Duplessy (2005), Changes in deep water hydrology during the Last Deglaciation, *C. R. Geosci.*, *337*, 919–927.

Lisiecki, L. E., and P. A. Lisiecki (2002), Application of dynamic programming to the correlation of paleoclimate records, *Paleoceanography*, *17*(D4), 1049, doi:10.1029/2001PA000733.

Lisiecki, L. E., and M. E. Raymo (2005), A Pliocene-Pleistocene stack of 57 globally distributed benthic δ^{18}O records, *Paleoceanography*, *20*, PA1003, doi:10.1029/2004PA001071.

Lisiecki, L. E., and M. E. Raymo (2009), Diachronous benthic δ^{18}O responses during late Pleistocene terminations, *Paleoceanography*, *24*, PA3210, doi:10.1029/2009PA001732.

Little, M. G., R. R. Schneider, D. Kroon, B. Price, T. Bickert, and G. Wefer (1997), Rapid paleoceanographic changes in the Benguela Upwelling System for the last 160,000 years as indicated by abundances of planktonic foraminifera, *Palaeogeogr. Palaeoclim. Palaeoecol.*, *130*, 135–161.

Liu, Z., et al. (2009), Transient simulation of last deglaciation with a new mechanism for Bølling-Allerød warming, *Science*, *325*, 310–314, doi:10.1126/science.1171041.

Lowe, D. J., P. A. R. Shane, B. V. Alloway, and R. M. Newnham (2008), Fingerprints and age models for widespread New Zealand tephra marker beds erupted since 30,000 years ago: A framework for NZ-INTIMATE, *Quat. Sci. Rev.*, *27*, 95–126.

Marcott, S. A., et al. (2011), Ice-shelf collapse from subsurface warming as a trigger for Heinrich events, *Proc. Natl. Acad. Sci. U.S.A.*, *108*(33), 13,415–13,419, doi:10.1073/pnas.1104772108.

MARGO Project Members (2009), Constraints on the magnitude and patterns of ocean cooling at the Last Glacial Maximum, *Nat. Geosci.*, *2*, 127–132, doi:10.1038/ngeo411.

Martinson, D. G., N. G. Pisias, J. D. Hays, J. Imbrie, T. C. Moore, and N. J. Shackleton (1987), Age dating and the orbital theory of the ice ages: Development of a high-resolution 0 to 300,000 year chronostratigraphy, *Quat. Res.*, *27*, 1–29.

Matsumoto, K., T. Oba, J. Lynch-Stieglitz, and H. Yamamoto (2002), Interior hydrography and circulation of the glacial Pacific Ocean, *Quat. Sci. Rev.*, *21*, 1693–1704.

Mignot, J., A. Ganopolski, and A. Levermann (2007), Atlantic subsurface temperatures: Response to a shutdown of the overturning circulation and consequences for its recovery, *J. Clim.*, *20*, 4884–4898.

Molyneux, E. G., I. R. Hall, R. Zahn, and P. Diz (2007), Deep water variability on the southern Agulhas Plateau: Interhemispheric links over the past 170 ka, *Paleoceanography*, *22*, PA4209, doi:10.1029/2006PA001407.

Nürnberg, D., N. Brughmans, J. Schönfeld, U. Ninnemann, and C. Dullo (2004), Paleo-export productivity, terrigenous flux, and sea surface temperature around Tasmania—Implications for glacial/interglacial changes in the Subtropical Convergence Zone, *Geophys. Monogr. Ser.*, *151*, 291–318.

Ohkushi, K., A. Suzuki, H. Kawahata, and L. P. Gupta (2003), Glacial-interglacial deep-water changes in the NW Pacific inferred from single foraminiferal δ^{18}O and δ^{13}C, *Mar. Micropaleontol.*, *48*, 281–290.

Oliver, K. I. C., B. A. A. Hoogakker, S. Crowhurst, G. M. Henderson, R. E. M. Rickaby, N. R. Edwards, and H. Elderfield (2010), A synthesis of marine sediment core δ^{13}C data over the last 150000 years, *Clim. Past*, *6*, 645–673, doi:10.5194/cp-6-645-2010.

Ostermann, D. R., and W. B. Curry (2000), Calibration of stable isotopic data: An enriched δ^{18}O standard used for source gas mixing detection and correction, *Paleoceanography*, *15*(3), 353–360.

Pahnke, K., and R. Zahn (2005), Southern Hemisphere water mass conversion linked with North Atlantic climate variability, *Science*, *307*, 1741–1746, doi:10.1126/science.1102163.

Pahnke, K., R. Zahn, H. Elderfield, and M. Schulz (2003), 340,000-year centennial-scale marine record of Southern Hemisphere climatic oscillation, *Science*, *301*, 948–952.

Pahnke, K., S. L. Goldstein, and S. R. Hemming (2008), Abrupt changes in Antarctic Intermediate Water circulation over the past 25,000 years, *Nat. Geosci.*, *1*(12), 870–874, doi:10.1038/ngeo360.

Peltier, W. R., and R. G. Fairbanks (2006), Global glacial ice volume and Last Glacial Maximum duration from an extended Barbados sea level record, *Quat. Sci. Rev.*, *25*, 3322–3337.

Piotrowski, A. M., S. L. Goldstein, S. R. Hemming, and R. G. Fairbanks (2004), Intensification and variability of ocean thermohaline circulation through the last deglaciation, *Earth Planet. Sci. Lett.*, *225*, 205–220.

Piotrowski, A. M., V. K. Banakar, A. E. Scrivner, H. Elderfield, A. Galy, and A. Dennis (2009), Indian Ocean circulation and productivity during the last glacial cycle, *Earth Planet. Sci. Lett.*, *285*, 179–189.

Pisias, N. G., D. G. Martinson, T. C. Moore, N. J. Shackleton, W. Prell, J. Hays, and G. Boden (1984), High resolution stratigraphic correlation of benthic oxygen isotopic records spanning the last 300,000 years, *Mar. Geol.*, *56*, 119–136.

Primeau, F., and E. Deleersnijder (2009), On the time to tracer equilibrium in the global ocean, *Ocean Sci.*, *5*, 13–28.
Rae, J. W. B., M. Sarnthein, G. L. Foster, A. Ridgwell, P. M. Grootes, and T. Elliott (2014), Deep water formation in the North Pacific and deglacial CO_2 rise, *Paleoceanography*, *29*, 645–667, doi:10.1002/2013PA002570.
Raymo, M. E., W. F. Ruddiman, N. J. Shackleton, and D. W. Oppo (1990), Evolution of Atlantic-Pacific $\delta^{13}C$ gradients over the last 2.5 m.y, *Earth Planet. Sci. Lett.*, *97*, 353–368.
Raymo, M. E., D. W. Oppo, B. P. Flower, D. A. Hodell, J. F. Mcmanus, K. A. Venz, K. F. Kleiven, and K. McIntyre (2004), Stability of North Atlantic water masses in face of pronounced climate variability during the Pleistocene, *Paleoceanography*, *19*, PA2008, doi:10.1029/2003PA000921.
Reimer, P. J., et al. (2013), IntCal13 and Marine13 radiocarbon age calibration curves, 0–50,000 years cal BP, *Radiocarbon*, *55*(4), 1869–1887.
Rühlemann, C., S. Mulitza, P. M. Muller, G. Wefer, and R. Zahn (1999), Warming of the tropical Atlantic Ocean and slowdown of thermohaline circulation during the last deglaciation, *Nature*, *402*, 511–514.
Rühlemann, C., et al. (2004), Intermediate depth warming in the tropical Atlantic related to weakened thermohaline circulation: Combining paleoclimate data and modeling results for the last deglaciation, *Paleoceanography*, *19*, PA1025, doi:10.1029/2003PA000948.
Sarnthein, M., K. Winn, S. J. A. Jung, J.-C. Duplessy, L. Labeyrie, H. Erlenkeuser, and G. Ganssen (1994), Changes in east Atlantic deepwater circulation over the last 30,000 years: Eight time slice reconstructions, *Paleoceanography*, *9*, 209–267, doi:10.1029/93PA03301.
Sarnthein, M., P. Grootes, J. Kennett, and M.-J. Nadeau (2007), ^{14}C reservoir ages show deglacial changes in ocean currents and carbon cycle, *Geophys. Monogr. Ser.*, *173*, 175–196, doi:10.1029/173GM13.
Schönfeld, J., R. Zahn, and L. de Abreu (2003), Surface and deep water response to rapid climate changes at the Western Iberian Margin, *Global Planet. Change*, *36*, 237–264.
Shackleton, N. J. (1974), Attainment of isotopic equilibrium between ocean water and the benthonic foraminifera genus *Uvigerina*: Isotopic changes in the ocean during the last glacial, *Cent. Natl. Rech. Sci. Coloq. Int.*, *219*, 203–209.
Shackleton, N. J., M. A. Hall, and E. Vincent (2000), Phase relationships between millennial-scale events 64,000–24,000 years ago, *Paleoceanography*, *115*(6), 565–569, doi:10.1029/2000PA000513.
Shakun, J. D., P. U. Clark, F. He, S. A. Marcott, A. C. Mix, Z. Liu, B. Otto-Bliesner, A. Schmittner, and E. Bard (2012), Global warming preceded by increasing carbon dioxide concentrations during the last deglaciation, *Nature*, *484*, 49–54, doi:10.1038/nature10915.
Siberlin, C., and C. Wunsch (2011), Oceanic tracer and proxy time scales revisited, *Clim. Past*, *7*, 27–39.
Siddall, M., et al. (2003), Sea-level fluctuations during the last glacial cycle, *Nature*, *423*, 853–858.
Sikes, E. L., C. R. Samson, T. P. Guilderson, and W. R. Howard (2000), Old radiocarbon ages in the southwest Pacific Ocean during the last glacial period and deglaciation, *Nature*, *405*, 555–559.
Skinner, L. C., and N. J. Shackleton (2005), An Atlantic lead over Pacific deep-water change across Termination I: Implications for the application of the marine isotope stage stratigraphy, *Quat. Sci. Rev.*, *24*, 571–580.
Skinner, L. C., S. Fallon, C. Waelbroeck, E. Michel, and S. Barker (2010), Ventilation of the deep Southern Ocean and deglacial CO_2 rise, *Science*, *328*, 1147–1151, doi:10.1126/science.1183627.
Smart, C. W., C. Waelbroeck, E. Michel, and A. Mazaud (2010), Benthic foraminiferal abundance and stable isotopic changes in the Indian Ocean sector of the Southern Ocean during the last 20 kyr: Paleoceanographic implications, *Palaeogeogr. Palaeoclimatol. Palaeoecol.*, *297*, 537–548.
Stern, J. V., and L. E. Lisiecki (2013), North Atlantic circulation and reservoir age changes over the past 41,000 years, *Geophys. Res. Lett.*, *40*, 3693–3697, doi:10.1002/grl.50679.
Stocker, T. F., and S. J. Johnsen (2003), A minimum thermodynamic model for the bipolar seesaw, *Paleoceanography*, *18*(4), 1087, doi:10.1029/2003PA000920.
Stocker, T. F., D. G. Wright, and W. S. Broecker (1992), The influence of high-latitude surface forcing on the global thermohaline circulation, *Paleoceanography*, *7*(5), 529–541, doi:10.1029/92PA01695.
Stocker, T. F., A. Timmermann, M. Renold, and O. Timm (2007), Effects of salt compensation on the climate model response in simulations of large changes of the Atlantic meridional overturning circulation, *J. Clim.*, *20*, 5912–5928.
Svensson, A., et al. (2008), A 60 000 year Greenland stratigraphic ice core chronology, *Clim. Past*, *4*(1), 47–57, doi:10.5194/cp-4-47-2008.
Thornalley, D. J. R., H. Elderfield, and I. N. McCave (2010), Intermediate and deep water paleoceanography of the northern North Atlantic over the past 21,000 years, *Paleoceanography*, *25*, PA1211 doi:10.1029/2009PA001833.
Van Kreveld, S., M. Sarnthein, H. Erlenkeuser, P. Grootes, S. Jung, M. J. Nadeau, U. Pflaumann, and A. Voelke (2000), Potential links between surging ice sheets, circulation changes, and the Dansgaard-Oeschger cycles in the Irminger Sea, 60-18 kyr, *Paleoceanography*, *15*(4), 425–442, doi:10.5194/cp-4-47-2008.
Vidal, L., R. R. Schneider, O. Marchal, T. Bickert, T. F. Stocker, and G. Wefer (1999), Link between the North and South Atlantic during the Heinrich events of the last glacial period, *Clim. Dyn. 15*, 909–919.
Venz, K. A., D. A. Hodell, C. Staton, and D. A. Warnke (1999), A 1.0 myr record of glacial North Atlantic Intermediate Water variability from ODP Site 982 in the northeast Atlantic, *Paleoceanography 14*, 42–52, doi:10.1029/1998PA900013.
Waelbroeck, C., C. Levi, J.-C. Duplessy, L. Labeyrie, E. Michel, E. Cortijo, F. Bassinot, and F. Guichard (2006), Distant origin of circulation changes in the Indian Ocean during the last deglaciation, *Earth Planet. Sci. Lett.*, *243*, 244–251.
Waelbroeck, C., L. C. Skinner, L. Labeyrie, J.-C. Duplessy, E. Michel, N. Vazquez Riveiros, J.-M. Gherardi, and F. Dewilde (2011), The timing of deglacial circulation changes in the Atlantic, *Paleoceanography*, *26*, PA3213, doi:10.1029/2010PA002007.
Wunsch, C., and P. Heimbach (2008), How long to oceanic tracer and proxy equilibrium?, *Quat. Sci. Rev.*, *27*, 637–651.
Xie, R. C., F. Marcantonio, and M. W. Schmidt (2012), Deglacial variability of Antarctic intermediate water penetration into the North Atlantic from authigenic neodymium isotope ratios, *Paleoceanography*, *27*, PA3221, doi:10.1029/2012PA002337.